Astron. Astrophys. 334, 863–872 (1998)

ASTRONOMY AND ASTROPHYSICS

The active RS Canum Venaticorum binary II Pegasi⋆

I. Stellar and orbital parameters

S.V. Berdyugina[1,2], **S. Jankov**[3], **I. Ilyin**[1], **I. Tuominen**[1], **and F.C. Fekel**[4]

[1] Astronomy Division, University of Oulu, P.O. Box 333, FIN-90571 Oulu, Finland (e-mail: sveta@ukko.oulu.fi)
[2] Crimean Astrophysical Observatory, P.O. Nauchny, Crimea, 334413 Ukraine
[3] Universidade de São Paulo, Depto. de Astronomia, C.P. 30627, São Paulo 01051, Brazil
[4] Center for Automated Space Science and Center of Excellence in Information Systems, Tennessee State University, Nashville, TN 37203, USA

Received 11 December 1997 / Accepted 5 March 1998

Abstract. A detailed model atmosphere analysis of high-resolution and high S/N CCD spectra of II Peg has yielded for the first time a self-consistent set of fundamental parameters of the primary component: $T_{\rm eff}$=4600 K, $\log g$=3.2, [M/H]=–0.4, $\xi_{\rm t}$=2.0 km s^{-1}. In addition, 121 new high quality radial velocity measurements[1] allowed us to determine improved orbital parameters, resulting in a new orbital ephemeris of $T_{\rm conj}$=2449582.9268+6.724333*E*. The position of the primary of II Peg in the HR diagram with the new parameters corresponds to a K2 IV star with mass ≈0.8 $M_\odot$. The evolved character of the star is confirmed by the C/N ratio, which is reduced significantly relative to the solar value. The unspotted V magnitude of the star of $6\overset{\rm m}{.}9$ is estimated from the observed variations of the TiO bands and quasi-simultaneous photometry. The blend of Li I 6707 Å is suspected to vary in equivalent width due to spot modulation. The lithium abundance for the unspotted star, Li/H=1.0±0.1, is found to be consistent with other post-main sequence chromospherically active stars. Combining all parameters, the radius R ≈ 3.4 $R_\odot$ and the inclination $i \approx 60^\circ$ of the primary are estimated with the assumption that its rotational axis is perpendicular to the orbital plane. The secondary is probably a M0-M3 V star with a mass of about 0.4 $M_\odot$.

Key words: stars: binaries: spectroscopic – stars: fundamental parameters – stars: abundances – stars: activity – stars: individual: II Peg

Send offprint requests to: S.V. Berdyugina

⋆ based on observations collected at the Nordic Optical Telescope (NOT), La Palma, Spain; the 2.6 m telescope of the Crimean Astrophysical Observatory, Ukraine; the 2.7 m and 2.1 m telescopes of the McDonald Observatory, USA; the coudé feed telescope of the Kitt Peak National Observatory, USA

[1] Table 2 is also available in electronic form at the CDS via anonymous ftp to cdsarc.u-strasbg.fr (130.79.128.5) or via http://cdsweb.u-strasbg.fr/Abstract.html.

1. Introduction

II Peg (HD 224085) was discovered to show periodic photometric variability by Chugainov (1976a). Now it is known as one of the most active RS CVn type stars, which are usually G-K subgiants or giants in close binaries. The periodic photometric variability of such stars is interpreted in terms of cool surface spots analogous to sunspots but much enhanced in scale. The existence of cool spots on the surface of II Peg is confirmed by the presence of TiO bands in the observed spectrum of the star (Vogt 1981).

Sanford (1921) obtained the earliest radial velocity measurements of the primary of II Peg and found that the orbit is nearly circular. Although the orbit was subsequently refined by several authors, the best previous ephemeris still predicts the radial velocities with an accuracy ±2.5 km s^{-1}, which is unsatisfactory for our purposes.

Several spectral types of the primary of II Peg have been determined, ranging between K0 and K3 in temperature, and between III and V in luminosity. Rucinski (1977) deduced a spectral type of K2-3 IV-V and noted some inconsistencies in the line ratios. The secondary of II Peg is unseen and probably a low-mass main sequence star.

For some time the presence of Li I 6707 Å line in the spectrum of II Peg was suggested to be an indication that the star must be rather young. Thus, because of its location slightly above the main sequence, the star was suggested to be in a late stage of pre-main sequence evolution (Rucinski 1977). However, Fekel & Balachandran (1993) and Randich et al. (1994) found the presence of substantial amounts of Li to be typical in many chromospherically active stars. The question is whether these relatively high Li abundances are due to enhanced chromospheric activity or rather are a consequence of the evolutionary history of the stars.

This first part of our study of II Peg is based primarily on new high-resolution spectroscopy of II Peg during 1994-1996. The main purpose of these observations was to produce new surface images of the primary, but we found it extremely useful to exploit them for (i) improving the orbital parameters, (ii)

determining new atmospheric parameters of the primary in a self-consistent way, and (iii) determining the evolutionary status of both components of the binary. The results of this study should be considered as input for the subsequent surface imaging of the primary of II Peg (Berdyugina et al. 1998a) and an analysis of its chromospheric activity (Berdyugina et al. 1998b). The structure of this paper is as follows. The observation and data reduction procedures are described in Section 2. Orbital parameters are determined in Section 3. Atmospheric parameters of the primary together with the lithium abundance and C/N ratio are presented in Section 4. The fundamental parameters of the components of II Peg are discussed in Section 5, and finally, Section 6 presents a summary of our work.

2. Observations and data reduction

Observations were carried out in 1994-1996 with the SOFIN échelle spectrograph (Tuominen 1992) fed by the 2.56 m Nordic Optical Telescope (NOT) at the Roque de los Muchachos Observatory, La Palma, Canarias. The data were acquired with the 2nd camera equipped with a CCD detector of 1152×298 pixels, yielding a wide spectral range (in 14 orders) of approximately 5500-8500 Å. For all observing runs the projected width of the slit was set to be $0\farcs5$ on the sky, providing a spectral resolving power $\lambda/\Delta\lambda \approx 83\,000$. With this setup, the dispersion at 6170 Å was 37 mÅ per pixel. A typical exposure time of $\approx 1^{\rm h}$ achieved a signal-to-noise ratio of more than 200 for most spectra. Additionally, one exposure of β Gem was obtained with the same setup to determine the velocity zero-point of the spectrograph and to use as a standard in spectrum synthesis calculations. It is a known standard star in both cases.

During the 1996 season II Peg was also observed with the coudé spectrograph installed on the 2.6 m telescope of the Crimean Astrophysical Observatory. The detector was CCD SDS 9000, Photometrics GmbH with 1024×400 pixels. With the slit of $0\farcs4$ and dispersion of 65 mÅ per pixel a resolving power as large as 41 000 was obtained. The covered spectral range was about 60 Å centered at 6170 Å or 7065 Å. The signal-to-noise ratio of an individual exposure was in most cases greater than 150.

From 1978 to 1980, 5 spectroscopic observations were obtained with the 2.7 m or 2.1 m telescopes, coudé spectrographs, and Reticon detectors at the McDonald Observatory. The spectra were centered at 6430 Å or 6700 Å, with $\lambda/\Delta\lambda$ = 20 000 and S/N $>$ 150. Observations were continued from 1990 to 1997 with the coudé feed telescope, coudé spectrograph, and a TI CCD at Kitt Peak National Observatory. Twenty spectra were centered at 6430 Å except for one at 6700 Å and one at 6565 Å, having $\lambda/\Delta\lambda$ = 30 000 and S/N $>$ 200. These observations were used only for the radial velocity measurements.

The reduction of the SOFIN data, described by Ilyin (1997), included bias, scattered light, and flat field corrections, extraction of spectral orders, and wavelength calibration. The latter is obtained with a thorium-argon comparison spectrum. Finally, the wavelengths were corrected for the Earth's motion. The Crimean spectra were reduced similarly except for the steps specifically relating to the echelle spectra.

Great care was taken in the continuum normalization, since the numerous photospheric lines are affected by the large rotational broadening, so the true continuum is not observed in almost all spectral regions. In the first iteration the continuum level was defined by a smoothing cubic spline drawn through estimated continuum points. In the next iteration the spectrograms were normalized to a common continuum level by comparing the observed spectra with a synthetic one, broadened to the same rotational velocity. In principle, it should suffice, if the synthetic spectrum describes perfectly the spectrum of the star. In any case, it could be improved after subsequent estimates of stellar parameters.

Table 1. Radial velocities of β Gem.

HJD	Order	$\lambda_{\rm c}$,Å	RV,km s^{-1}
2450383.7681	34	6725	3.52
”	35	6534	3.74
”	36	6353	3.74
”	37	6181	3.57
”	39	5864	3.60
		Mean =	3.63±0.04

3. Parameters of the orbit

3.1. Zero-point velocity of the SOFIN spectrograph

To estimate the zero-point velocity of the SOFIN spectrograph, we measured the radial velocity of β Gem (HD 62509), which is recommended as a standard radial velocity star with RV=+3.3±0.1 km s^{-1}(Astronomical Almanac 1997). The RV of β Gem was measured by cross-correlating observed spectra with synthetic ones for five orders containing strong absorption lines. The source of line lists was the Vienna Atomic Line Database (hereafter VALD, Piskunov 1995), and stellar parameters were taken from the detailed model atmosphere analysis of the star by Drake and Smith (1991). The results of the measurements are presented in Table 1. There are no significant differences among radial velocities measured from different orders nor is there a systematic trend with wavelength. Thus, comparing the mean value with the assumed one, we deduce the *instant* zero-point velocity correction of the SOFIN spectrograph of 0.3±0.1 km s^{-1}. We call it *instant* because this is only a measurement of that value at a certain moment. In reality the correction might be a more complicated function. It should be stressed that we did not take into account the determined velocity correction in the subsequent reduction, but we wanted only to estimate how large it is.

3.2. A log of RV measurements of II Peg

We have obtained a total of 121 new observations (59 from SOFIN, 37 from Crimea, 5 from McDonald, and 20 from KPNO), and the data sets have rather good phase coverage.

The SOFIN observations have velocities measured from several orders, increasing the accuracy of those radial velocity measurements. Unfortunately, many of the 14 orders could not be used because numerous atmospheric lines in some wavelength regions strongly disturb the cross-correlation function.

The radial velocities of II Peg from the SOFIN and Crimean data were measured by cross-correlating the observed spectra with the synthetic spectra calculated with appropriate atmospheric parameters. Probably, such a procedure is more accurate than using a standard-star spectrum due to the possible inconsistency of relative strengths of lines and, therefore, shapes of rotationally broadened blends. Furthermore, the RV measurements could be improved after the new stellar parameters were determined. Also, note that the line list for the spectra calculations was improved using the spectrum of β Gem (this procedure is discussed in Section 3 as well). From the SOFIN data we used spectra of seven orders: the orders given in Table 1 as well as the 27th (λ_c=8440 Å) and the 41st (λ_c=5560 Å). Again, we found no significant systematic velocity trend among orders spanning wavelengths from 5560 to 8440 Å.

The McDonald and KPNO spectra were measured with the cross-correlation procedure of Fitzpatrick (1993). However, only the least blended 3 or 4 lines were used. In some cases the correlation profile was obviously asymmetric. In such cases the fits emphasized the shoulders rather than the center of the profile. Velocities were determined relative to the IAU standard stars ι Psc, α Ari, or HR 8551, whose velocities were taken from Scarfe et al. (1990). Also used as standards were μ Her (Stockton & Fekel 1992) and β Aql, the latter tied to the IAU system and having an assumed velocity of –40.2 km s^{-1}.

Earlier radial velocity measurements of II Peg, 25 RVs from Sanford (1921), 6 RVs from Halliday (1952), 1 RV from Heard (1956), 2 RVs from Rucinski (1977), and 2 RVs from Vogt (1981), were used in the period determination. So, the available data presently consists of 157 values, spanning from 1917 to 1997. Thus, we have a fortunate opportunity to derive new, much more accurate, orbital parameters of II Peg. We suspect that the presentation of the whole log of the measurements in Table 2 is relevant for both the present discussion and the future.

3.3. The orbit

For our purpose we used the program FOTEL3 developed by Hadrava (1995), which is able to deduce the orbital period value together with other parameters for both circular and eccentric orbits. The first step was to determine new values of the period P and eccentricity e. A first solution was found for all radial velocity measurements listed in Table 2 with appropriate weights which were determined from the variances to the fit. It is given in Table 3. Note that the fit allowed different γ-velocities for different data sets. In comparison to the previous published values of P and e by Vogt (1981) the new values are much more accurate. Moreover, if only new RVs are used to determine the eccentricity, then it drops to 0.0025±0.0026. Such a small value of the eccentricity could be probably ignored for the present, and the orbit can be considered as circular.

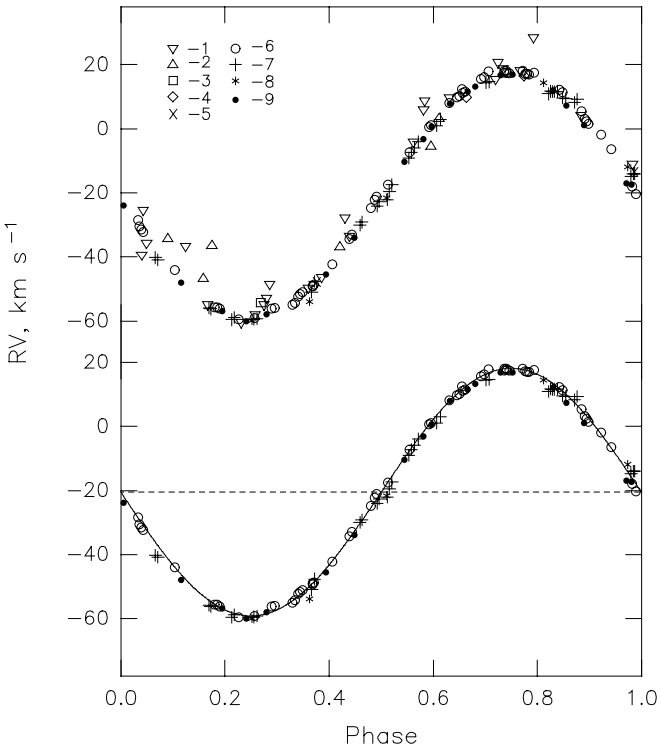

Fig. 1. Radial velocity measurements phased with the new ephemeris T_{conj} = 2449582.9268 + 6.724333 E. The top displays all measurements with the same reference numbers as in Table 2, while the bottom shows the new data only with the Solution 2 as a solid line (see Table 3).

The accuracy of the data sets is obviously rather different, and the new measurements are significantly more accurate, especially the SOFIN data. For this reason we assumed the period from the all-data solution and the eccentricity to be zero and found the best solution from the new data appropriately weighted. Two solutions are given in Table 3, and the measurements phased with the ephemeris T_{conj} = 2449582.9268 + 6.724333 E are shown in Fig. 1.

4. Atmospheric parameters of the primary

4.1. Inputs for spectra calculations

A list of atomic line parameters for a given wavelength region was obtained from VALD for lines having a central depth of 1% or more.

A number of molecular lines were added to the list, since the presence of many molecular lines in spectra of stars with effective temperature T_{eff}<5000 K is quite noticeable. Although weaker than most atomic lines, they are so numerous that they can effectively reduce the continuum level in spectra of rapidly rotating stars. In those regions that we used for our study the most significant contribution to the photospheric spectrum from molecular lines is due to rotational transitions of a number of vibrational bands of the CN ($A^2\Pi - X^2\Sigma$) red system. The main sources of the CN line parameters are the following: wavelengths are from laboratory measurements by Davis & Phillips

Table 2. Radial velocities (RV, km s^{-1}) data. References (ref): 1 - Sanford (1921); 2 - Halliday (1952); 3 - Heard (1956); 4 - Rucinski (1977); 5 - Vogt (1981); 6 - SOFIN; 7 - Crimea; 8 - McDonald; 9 - KPNO.

HJD 2400000+	RV	ref	HJD 2400000+	RV	ref	HJD 2400000+	RV	ref	HJD 2400000+	RV	ref	HJD 2400000+	RV	ref
21441.480	–11.1	1	43031.914	16.6	4	50295.592	–18.0	6	50289.463	–40.9	7	50403.191	–14.0	7
21556.196	–25.5	1	43037.888	9.9	4	50295.640	–20.3	6	50290.419	–59.5	7	50403.209	–13.9	7
21592.126	–46.5	1	43362.823	–13.1	5	50297.658	–56.2	6	50290.451	–58.8	7	50409.158	8.3	7
21823.489	28.5	1	43452.864	–47.4	5	50297.697	–56.0	6	50291.449	–51.0	7	50409.194	9.3	7
21833.454	–55.0	1	49578.684	–49.0	6	50298.657	–34.3	6	50291.488	–47.7	7	43744.942	14.4	8
21860.387	–53.0	1	49579.654	–17.5	6	50298.696	–33.0	6	50292.423	–22.1	7	44474.870	–53.9	8
22216.449	–60.5	1	49580.608	12.5	6	50299.686	0.6	6	50292.455	–19.5	7	44475.870	–21.6	8
22533.360	–49.7	1	49581.543	17.6	6	50299.714	1.1	6	50292.487	–17.4	7	44478.983	–11.9	8
22541.442	–4.2	1	49582.541	–6.4	6	50381.354	17.5	6	50297.427	–59.5	7	44480.855	–59.9	8
22565.392	–36.7	1	49583.627	–44.1	6	50381.386	17.6	6	50297.466	–59.2	7	48060.983	11.6	9
22566.480	–48.6	1	49584.655	–59.1	6	50381.421	17.4	6	50299.428	–9.1	7	48427.968	–60.0	9
22567.513	–33.5	1	49585.661	–42.3	6	50382.390	03.2	6	50299.462	–7.3	7	49620.799	7.9	9
22568.470	5.9	1	49586.659	–7.3	6	50382.414	02.4	6	50300.422	14.5	7	49901.986	–33.9	9
22569.398	15.4	1	49587.679	17.9	6	50382.438	01.5	6	50300.464	14.7	7	49902.991	0.7	9
22593.191	–58.1	1	49910.656	18.1	6	50383.361	–30.5	6	50301.417	9.6	7	49903.879	16.7	9
22594.353	–27.9	1	49910.677	18.0	6	50383.389	–31.5	6	50301.458	9.4	7	49968.868	–45.5	9
22595.380	8.6	1	49911.645	5.5	6	50383.409	–32.3	6	50312.468	–24.0	7	49969.881	–10.3	9
22596.327	20.6	1	49912.645	–28.4	6	50384.366	–55.6	6	50312.496	–22.7	7	49970.790	13.2	9
22624.297	4.2	1	49913.631	–55.6	6	50384.407	–56.1	6	50348.301	10.9	7	49971.801	12.0	9
22625.348	–39.4	1	49914.636	–55.0	6	50385.414	–52.3	6	50348.332	11.7	7	49972.814	–17.3	9
22626.203	–55.0	1	49914.675	–54.3	6	50385.443	–51.6	6	50348.351	11.6	7	49973.721	–48.0	9
22629.318	9.7	1	49915.655	–24.7	6	50385.472	–51.0	6	50353.299	–5.9	7	50263.973	–57.9	9
22630.235	18.2	1	49916.664	8.1	6	50386.402	–22.2	6	50353.347	–3.9	7	50265.994	–3.2	9
22650.187	18.8	1	49917.614	18.0	6	50386.430	–21.1	6	50357.368	–55.9	7	50362.762	–17.0	9
22652.308	–35.8	1	49918.626	–1.9	6	50387.468	9.7	6	50357.389	–56.2	7	50401.635	16.9	9
32100.731	–46.7	2	49920.668	–59.5	6	50387.499	10.2	6	50359.314	–30.0	7	50404.609	–56.9	9
32873.567	–34.2	2	49921.627	–49.3	6	50387.536	11.2	6	50359.341	–29.1	7	50630.951	7.3	9
33149.836	–36.4	2	49921.645	–48.7	6	50387.569	11.5	6	50360.309	1.0	7	50631.961	–23.9	9
33199.733	–5.4	2	50293.634	15.6	6	50388.348	17.2	6	50360.352	3.0	7	50637.908	1.1	9
33507.881	–36.8	2	50293.676	16.2	6	50388.376	17.0	6	50402.171	11.5	7			
33542.779	3.3	2	50294.647	12.2	6	50388.401	16.9	6	50402.210	11.7	7			
34266.707	–54.2	3	50294.690	11.3	6	50289.431	–40.2	7	50403.164	–14.8	7			

Table 3. The results of two orbit solutions. The best one is from the new data only. The reference code for different γ-velocities listed in Solution 1 is the same as for Table 2.

Element	Solution1, all RVs		Solution2, New RVs	
P, days	6.724333	±0.000010	6.724333	
e,	0.0065	±0.0055	0.0	
K_1, km s^{-1}	38.36	±0.22	38.66	±0.13
$a_1 \sin i$, $R_\odot$	5.1		5.2	
f_1(m), $M_\odot$	0.03939		0.04028	
T_{maxRV}, HJD	2449581.2500	±0.0048	2449581.2457	±0.0039
T_{conj}, HJD	2449582.9220	±0.0048	2449582.9268	±0.0039
γ, km s^{-1}	–17.8	±1.0 (1)	–20.5	±0.1
	–16.2	±2.7 (2,3)		
	–22.1	±0.6 (4)		
	–18.5	±1.3 (5)		
	–20.5	±0.1 (6)		
	–21.5	±0.3 (7)		
	–21.9	±1.0 (8)		
	–21.8	±0.2 (9)		

(1963); band oscillator strengths and molecular constants are from the RADEN database (Kuznetzova et al. 1993); lower level excitation energies and rotational intensity factors are calculated with formulas from the book by Kovacs (1969).

Stellar model atmospheres used are from Kurucz (1993). When necessary, a model with specific parameters was obtained from the grid by simple parabolic interpolation using three appropriate points in both effective temperature and surface gravity for a given metallicity. A code used for the synthetic spectrum calculations is described in detail by Berdyugina (1991). It includes calculations of opacities, intensities and fluxes in the continuum and atomic and molecular lines. Also, number densities of atoms and molecules are calculated under the assumption of dissociative equilibrium.

4.2. The standard star fit

As mentioned previously, β Gem (K0 IIIb) was chosen as a standard star for both radial velocity measurements and synthetic spectrum calculations. Although it is somewhat more luminous than the primary of II Peg, we obviously can use its spectrum to check most of our inputs for the synthetic spectrum calculations. Using the parameters of the star determined by Drake & Smith (1991) from a very detailed analysis, we have interpolated a model with $T_{\rm eff}$=4865 K and $\log g$=2.75 from the model grid. Other known parameters are the iron abundance [Fe/H]=–0.04 (assuming the solar value Fe/H=7.50 in scale of H=12), the calcium abundance Ca/H=6.25, microturbulence $\xi_{\rm t}$=1.4 km s^{-1}, and broadening due to the combined effects of rotation and macroturbulence, represented by a Gaussian function with width of 3.5 km s^{-1}. Note that the iron abundance was determined using 'solar' oscillator strengths. Additionally, the carbon, nitrogen and oxygen abundances were adopted at first as C/H=8.30, N/H=8.14, O/H=8.78 in accordance with Kjaergaard et al. (1982).

First calculations of the β Gem spectrum revealed a number of 'missing' and 'wrong' atomic lines in the input line list. For the CN lines, increasing the nitrogen abundance N/H by 0.1 dex resulted in a very good fit. Since accurate and reliable oscillator strengths are not available for the complete set of atomic lines used in the calculations, we tried to model the standard star's spectrum to derive 'stellar oscillator strengths' and used them in the subsequent analysis of the II Peg spectrum. Such a differential analysis also was used to avoid (or reduce) non-LTE effects in lines of the neutral atoms. Obviously, the set of the 'stellar oscillator strengths' cannot be considered a unique one because it contains uncertainties due to both the stellar parameters of the standard star and the stellar model used. Moreover, the latter is impossible to avoid in any case but can be reduced in the differential analysis. Unfortunately, some missing lines in the line list have not been identified even in the solar spectrum, where they are observed as well but are very weak. We stress that the final input line list is very important for our subsequent study, when we apply the surface imaging technique to the spectrum of II Peg.

Table 4. Measured projected rotational velocity

Season	Profile Fe I λ,Å	$v \sin i$ km s^{-1}
1994	6173.341	22.4
1994	6180.203	22.6
1995	6173.341	22.7
1995	6180.203	22.8
	Mean =	22.6

4.3. The rotational velocity and macroturbulence.

To determine the projected rotational velocity, $v \sin i$, of the primary, we used the profiles of the Fe I 6173.341 Å and 6180.203 Å photospheric absorption lines extracted from the average SOFIN spectra for two seasons: 1994 and 1995. Though the first line is magnetically sensitive, the expected strength of the magnetic field will not disturb its profile so that it may affect our results. The profiles and their Fourier transforms are shown in Fig. 2. The measured projected velocities, corresponding to a linear limb darkening coefficient of ε=0.7 (Al-Naimiy 1978), are given in Table 4. The first zero of the Fourier transform of the rotational profile was chosen for the projected rotational velocity measurements, since it is less affected by noise and small-scale intrinsic variability. To determine the macroturbulence, $\zeta_{\rm t}$, the synthesized profile has previously been convolved with the instrumental profile. Being less affected by noise, the first and second lobes of the Fourier transform of the observed mean profiles have been better fitted with the same value of an isotropic Gaussian macroturbulence of 4 km s^{-1}. The small residuals of the measured radial velocities along with the linear form of the bisector show that all deformations in individual profiles have been well averaged in the mean profiles. However, note that the positions of the second and third zeros of the rotational profile indicate that the observed linear limb darkening coefficient is less than its theoretical value. This would imply a lower projected rotational velocity together with a higher macroturbulence (of about 1-2 km s^{-1}). The projected rotational velocity of 23.1 $\pm$1.0 found by Fekel (1997) from 4 of the KPNO spectra is in excellent agreement with our SOFIN value of 22.6 km s^{-1}.

4.4. The parameters of the atmosphere

About 20 lines of different elements were chosen from those regions where the spot contribution to the spectrum appears to be insignificant. Since the equivalent widths of most lines do not display noticeable variation with phase, the average SOFIN spectrum of II Peg has been used in the analysis. At first, spectra of II Peg were averaged separately for the three seasons: 1994, 1995, and 1996. But no significant differences were found among them, and so the total averaged SOFIN spectrum of II Peg was used.

To obtain a self-consistent set of parameters we used the following procedure.

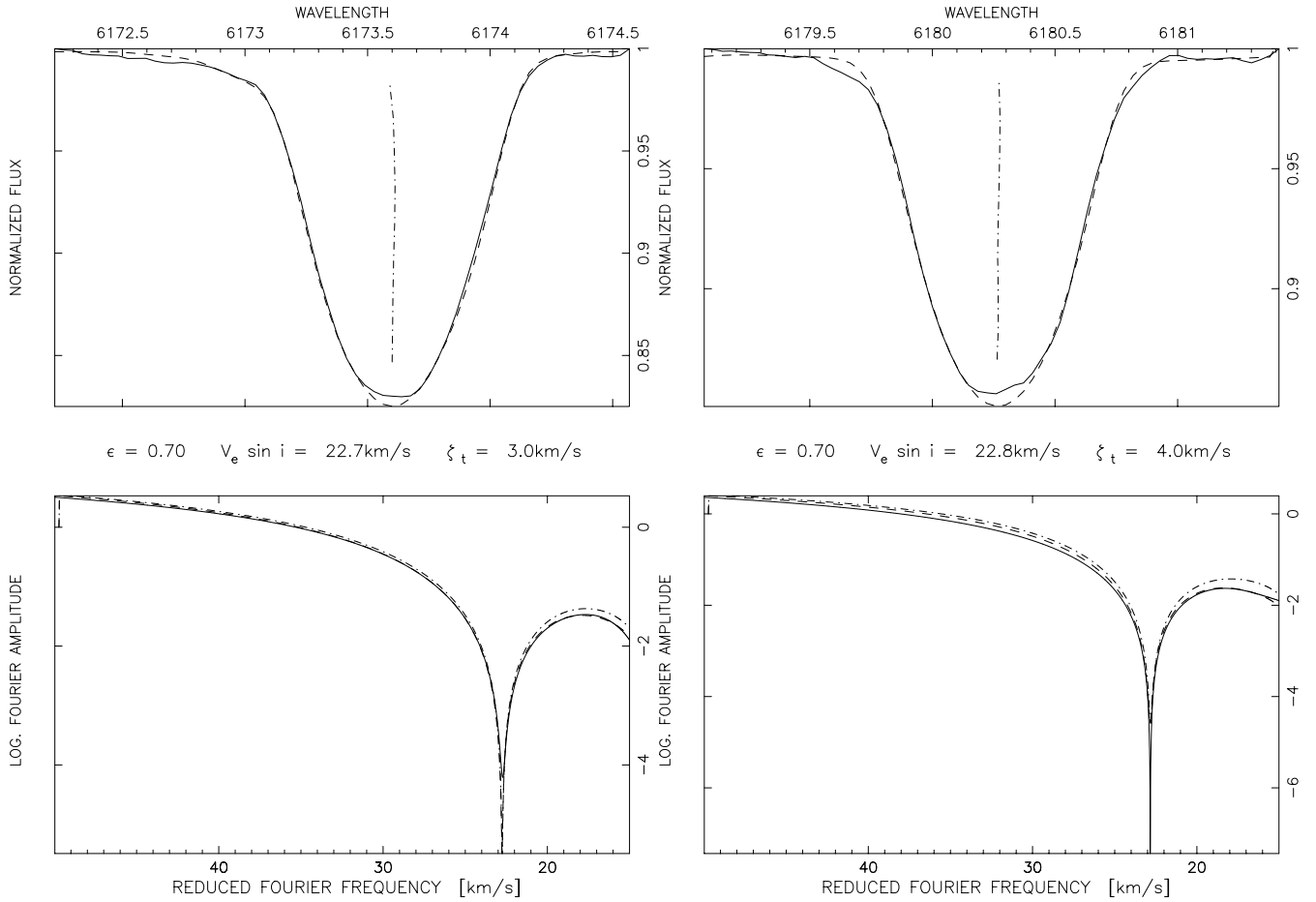

Fig. 2. Observed profiles (upper panels) of Fe I lines at 6173.341 Å (left) and 6180.203 Å (right) and their Fourier transforms (bottom panels). The dash-dotted line presents the Fourier transform of the rotationally broadened synthetic spectrum without macroturbulence, while the dashed line presents the profile with macroturbulence of 3 and 4 km s^{-1}.

1. Assuming first an appropriate pair of $T_{\rm eff}$ and $\log g$, we analyzed neutral metal lines to produce a set of curves (loci of constant equivalent width) on a diagram of metal abundance, [M/H], as a function of microturbulence, $\xi_{\rm t}$. The curves intersect in a narrow region which provides the initial estimate for [M/H] and $\xi_{\rm t}$ (Fig. 3a). Note that 'loci of constant equivalent width' in the sense of the synthetic spectrum calculations means the best fit to the observed spectrum.

2. Using the initial estimates of [M/H] and $\xi_{\rm t}$, we analyzed both neutral and ionized metal lines to produce a set of curves on a diagram of $T_{\rm eff}$ versus $\log g$. Since lines of ionized metals are sensitive to both parameters, and lines of neutral metals are sensitive mostly to temperature, the intersection region gives an initial estimate of a pair of $T_{\rm eff}$ and $\log g$ values (Fig. 3b).

3. The previous two stages were iterated until a self-consistent set of parameters was obtained. The results are given in Table 5.

Table 5. Atmospheric parameters of the primary of II Peg

Parameter	Value
$T_{\rm eff}$, K	4600±100
$\log g$	3.2±0.2
[M/H]	–0.4±0.1
$\xi_{\rm t}$, km s^{-1}	2.0±0.5
$\zeta_{\rm t}$, km s^{-1}	3.5±0.5
$v \sin i$, km s^{-1}	22.6±0.5

4.5. The lithium abundance

The lithium equivalent width has been measured by several authors. Chugainov (1976b) estimated a lithium abundance of Li/H=1.5 from a blend of 0.110 Å and claimed that the age of the star should be less than 1 Gyr. Rucinscki (1977) measured the equivalent width of the blend to be 0.055±0.010 Å and suggested that the star might be in a late stage of pre-main sequence evolution. Vogt (1981) has reported the observed feature at 6707.8 Å with an equivalent width of 51±1 mÅ to be clearly a blend of three lines: Fe I 6707.4 Å, Li I 6707.8 Å, and V I 6708.1 Å. Thus, the pure lithium equivalent width must be somewhat less than 51 mÅ.

Our results show the equivalent width of the blend ranging from 53 mÅ to 65 mÅ in 1994-1996 (with the accuracy of ±2

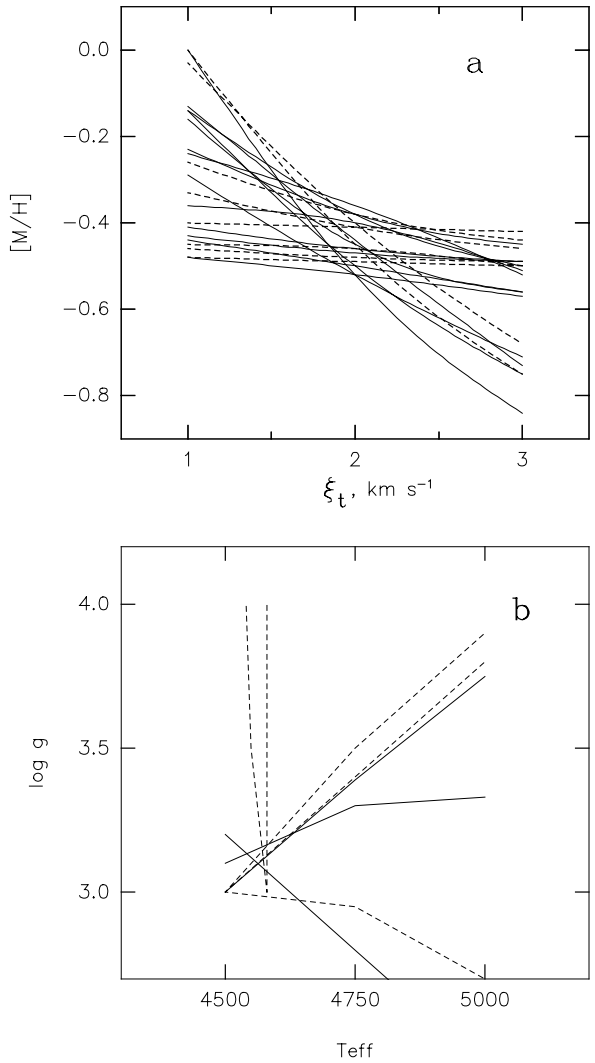

Fig. 3a and b. Diagrams for the self-consistent determination of the atmospheric parameters of the primary of II Peg: **a** metallicity [M/H] and microturbulence ξ_t, **b** effective temperature $T_{\rm eff}$ and surface gravity $\log g$. Solid curves are due to iron lines, and dashed ones are due to other metals.

mÅ), which with our new atmospheric parameters corresponds to a Li/H abundance range of 1.0 to 1.1 (Fig. 4). Using quasi-simultaneous photometric observations (Jetsu 1996, Berdyugin 1997) and simultaneous measurements of the central depth of the TiO bands at 7054 Å and 7125 Å we investigated whether the lithium equivalent width correlates with the spot coverage of the stellar disk. Giampapa (1984) predicted that chromospherically active stars would have significant variations in the strength of the lithium line as the size of the spot area on the visible hemisphere changes during a rotation cycle. Several groups, including Patterer et al. (1993) and Martin & Claret (1995), have examined lithium in pre-main sequence stars and claimed to have detected lithium equivalent width variations. Jeffries et al.'s (1994) observations of the young K dwarf BD+22 4409 have provided the most convincing evidence linking lithium equivalent width changes to changes in spot area. Fekel (1996) reviewed the relationship between spots and lithium equivalent width variations. He concluded that significant variations are not likely to be detected except in the most active stars that have significant contrast between the spotted and unspotted hemispheres. II Peg is indeed one of the most active known RS CVn binaries. But even in its case the variations are less than 25%, and a correlation with the brightness of the star is not quite evident (Fig. 4), although it probably exists. In fact, such a correlation seems to be disturbed by other effects. To estimate the unspotted V magnitude of the star, the variations of the central depth of the TiO bands at 7054 Å and 7125 Å are plotted versus photometric measurements in Fig. 4. The presence of TiO bands in the spectrum of II Peg is not compatible with its spectral class, and the bands are usually interpreted as originating in the regions of cool spots. From the linear regressions fitted to the data we estimate that at the historical brightness maximum of V=$7\overset{\rm m}{.}2$ the central depths of the TiO bands would be ≈1–2%. Extrapolating the TiO regressions to the zero value of the central depths provides an estimate of the V magnitude of $6\overset{\rm m}{.}9$ for the star with no spots. Similarly, Neff et al. (1995) concluded that at the historical brightness maximum at least 35% of the surface was covered with spots, and the V magnitude corresponding to the unspotted star should be equal to $6\overset{\rm m}{.}8$. For the lithium blend the extrapolation to the $6\overset{\rm m}{.}9$ magnitude gives an equivalent width of about 55±5 mÅ. Thus, taking into account all uncertainties, we conclude that the true value of the lithium abundance Li/H is about 1.0±0.1, and the spot contribution can be responsible only for 10-20% of the equivalent width of the blend.

The lithium abundance in conjunction with other stellar parameters is known to be a stellar age indicator. K0–K2 zero-age main sequence dwarf field stars have Li/H = 2.8–3.0 (Ambruster et al. 1994), nearly equal to that found in late-type pre-main sequence stars (Basri et al. 1991). Lithium abundances determined for such young field stars and T Tauri stars indicate that the equivalent widths and the corresponding abundances found for II Peg are inconsistent with a pre-main sequence evolutionary state. Fekel & Balachandran (1993) and Randich et al. (1994) have shown that moderate lithium abundances of 1.0–2.0 are found in a number of post-main sequence chromospherically active stars. Thus, the lithium abundance of II Peg appears to be quite consistent with such results. Its post-main sequence evolutionary state, discussed in section 5, is also confirmed by the observed C/N ratio (section 4.6).

4.6. The C/N ratio

A good criterion for the evolutionary state of a star is the C/N ratio (abundance ratio in the linear scale). For young or main sequence stars the C/N ratio should be close to the solar value of 4.8, while more evolved stars after the first dredge-up should display a much lower ratio, which depends slightly on the initial mass. For example, two K1 subgiants studied by Lambert&Ries (1981) show C/N ratios of 2.95 and 2.34. To determine this ratio for the primary of II Peg, the head of the (2,0) band of the CN red system was modelled with different amounts of carbon, while abundances of oxygen and nitrogen were set to the typical values

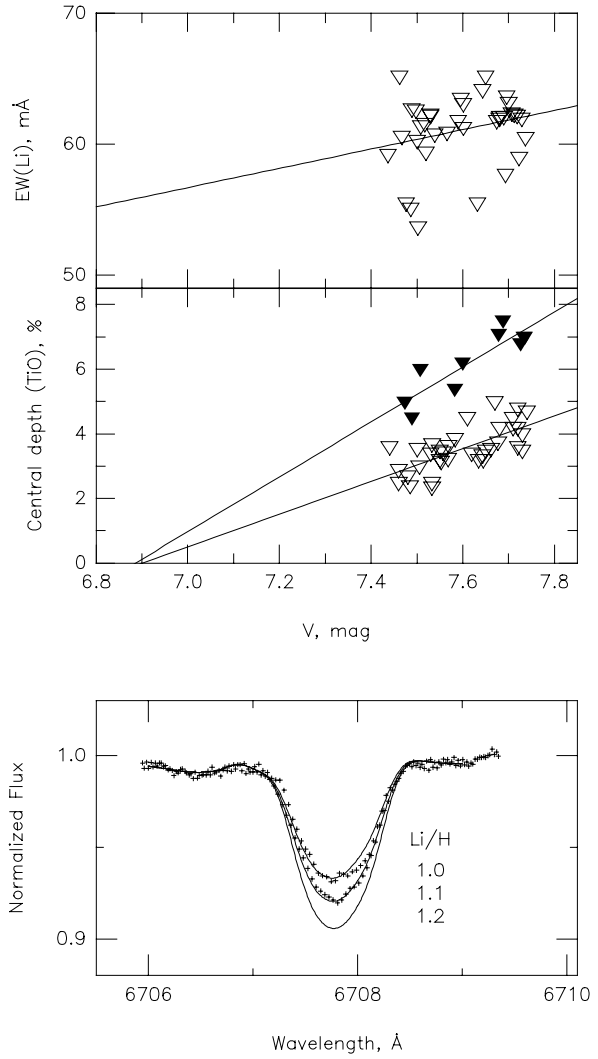

Fig. 4. The variation of the equivalent width of the 6707 Å blend and the central depth of the TiO band at 7125 Å in 1994-1996 (light triangles) and the TiO band at 7054 Å in 1996 (filled triangles) with V magnitude (top). At the bottom the lithium blend at the minimum (55 mÅ) and maximum (65 mÅ) equivalent width observed in 1994-1996 (symbols) and synthetic spectra calculated with three values of Li/H (lines).

for low metallicity subgiants: [O/H]=0.5·[Fe/H] (Clegg et al. 1981) and [N/H]=+0.24 (Lambert&Ries 1981). The reduced C/N ratio of ≤ 2 (Fig. 5) confirms the presence of processed CN-cycle matter in the atmosphere of the primary and, thus, its post-main sequence state.

5. Fundamental parameters of the components

The determined projected rotational velocity and the photometric period of the star (Strassmeier et al. 1993) result in the relation $R_1 \geq 3.0 R_\odot$. This corresponds to the radius of a subgiant star. The evolved character of the star is confirmed by the reduced C/N ratio estimated in Section 4. In addition, the galactic velocity-components indicate that II Peg is an old disk object (Eggen, 1978). With the new parallax value of $0\farcs02362$ from

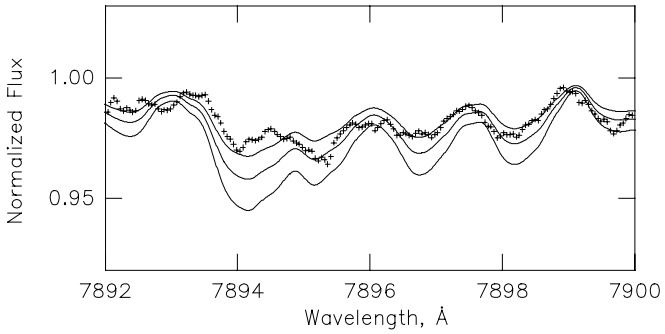

Fig. 5. The spectrum modelled in the region of the head of the (2,0) band of the CN red system. The observed spectrum is shown with symbols, while the lines are the calculated spectra with different values of the C/N ratio: 2.75, (the deepest one), 2.2, and 1.74 (the most shallow one).

the Hipparcos Catalogue (Perryman et al. 1997) and an unspotted visual magnitude of the star of $6\fm9$, an absolute magnitude $M_v = 3\fm8$ is determined. This value is significantly above that for main sequence stars of the same effective temperature ($M_v = 7\fm0$), less than that of giants ($M_v = 0\fm6$), and very close to the value of $3\fm1$ for cool subgiants (Lang 1992). Thus, there is no doubt that the primary of II Peg has evolved from the main sequence to the base of the red-giant branch. Then, the mass of the primary should be in the range of 0.7–1.1 $M_\odot$, where the lower limit corresponds to a main sequence star with $T_{\rm eff}$=4600K, while the upper limit is for a giant with the same temperature (Lang 1992). The corresponding ranges for the stellar radius and the inclination of the rotational axis are 3.5–4.4 $R_\odot$ and 60°–40°, respectively.

Since with present observing techniques the secondary is invisible at all wavelengths, its luminosity should be at least 100 times less than that of the primary, i.e. $M_v \leq 8\fm8$. This corresponds to a M0 main sequence star with a mass of 0.5 $M_\odot$. From the mass-mass diagram calculated with the mass function for various combinations of mass and orbital inclination (Fig. 6), narrower ranges for the radius and the inclination of the rotational axis of the primary can be found under the assumption that its rotational axis is perpendicular to the orbital plane. From a sample of synchronously rotating RS CVn binaries with similar periods, Glebocki & Stawikowski (1995) found that such an assumption is justified. The upper limit for the radius, then, drops to 3.8 $R_\odot$, while the lower limit for the stellar inclination grows to 53°. One can see that the upper limit for the mass of the secondary and the assumption of the perpendicularity of the rotational axis to the orbital plane significantly reduce the probable domain of the parameters of the binary, though they are still consistent. Then, for $\log g$= 3.2–3.4 the parameters are the following: $M_1/M_\odot = 0.8 \pm 0.1$, $M_2/M_\odot = 0.4 \pm 0.1$, $R_1/R_\odot = 3.4 \pm 0.2$, $i = 60° \pm 10°$. Scaltriti et al. (1990) attempted to estimate the orbital inclination from the linear polarization measurements. Unfortunately, the amplitude of the variability was comparable with the errors of the measurements, which resulted in a biased estimate of the inclination of 75°. The absence of the variability would be interpreted as an orbital inclination of 90° in that model. Additionally, the confidence level of that

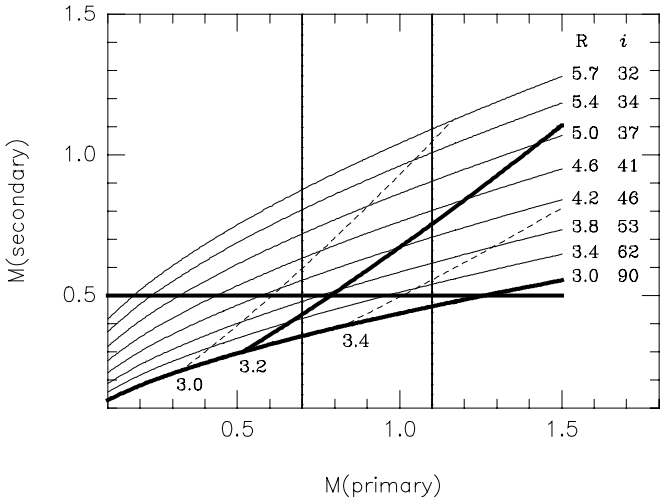

Fig. 6. The mass-mass diagram for II Peg (in solar units). The thin solid curves are calculated for the fixed values of the radius of the primary and the inclination (numbers in the left). The dashed lines are loci of the primary with a fixed value of log g (numbers at the bottom). The heavy solid lines show the boundaries with log g=3.2, R_1=3.0 $R_\odot$, and M_2=0.5 $M_\odot$, while the vertical lines are the boundaries for the mass of the primary (see text).

estimate is from 0° to 80° in accordance with Wolinski & Dolan (1994). Therefore, the estimate of 75° can be considered only as the highest possible inclination of the orbit.

6. Conclusions

From new high-resolution and high S/N spectra of II Peg, the following results have been obtained:

1. New orbital parameters have been determined, the ephemeris being improved: $T_{\rm conj}$ = 2449582.9268 + 6.724333E.

2. A detailed model atmosphere analysis of the spectrum of II Peg has yielded for the first time a self-consistent set of fundamental parameters of the primary component: $T_{\rm eff}$=4600 K, log g=3.2, [M/H]=–0.4, $\xi_{\rm t}$=2.0 km s^{-1}.

3. The blend of Li I 6707 Å is suspected to vary in equivalent width due to spot modulation. The lithium abundance for the unspotted star was determined: Li/H=1.0±0.1. It is found to be consistent with the lithium abundances in other post-main sequence chromospherically active stars.

4. An unspotted V magnitude of $6\overset{\rm m}{.}9$ was estimated from the observed variations of the TiO bands and quasi-simultaneous photometry.

5. With our new parameters the position of the primary of II Peg in the HR diagram corresponds to a K2 IV star with mass 0.8±0.1 $M_\odot$. The evolved character of the star is confirmed also by the C/N ratio, which is reduced significantly relative to the solar value.

6. By combining all parameters, the radius R_1 = 3.4±0.2 $R_\odot$ and the inclination i=60°±10°of the primary have been estimated with the assumption that its rotational axis is perpendicular to the orbital plane.

7. The unseen secondary is believed to be a M0-M3 main sequence star with a mass of about 0.4±0.1 $M_\odot$.

Acknowledgements. The research described in this publication was made possible in part by grants R2Q000 and U1C000 from the International Science Foundation and by grant A-05-067 from the ESO C&EE Programme. The work by S.B. was supported by a grant from the Centre for International Mobility (CIMO), Finland. F.C.F has been supported in part by NASA grants NAG8-1014 and NCC5-228 plus NSF grant HRD-9550561. We are grateful to Dr. Sumner Davis for the computer-readable catalogue of laboratory wavelengths of TiO and CN lines and to Dr. Ludmila Kuznetsova who provided the band oscillator strengths and molecular constants from the RADEN database. Dr. Rudolf Duemmler is acknowledged for discussions.

References

Al-Naimiy H.M, 1978, Ap&SS 53, 181
Ambruster C.W., Brown A., Fekel F.C., 1994, The 8 Cambridge Workshop on Cool Stars Stellar Systems, and the Sun, ASP Conf. Ser., Vol. 64, p. 348
Basri G., Martin E.L., Bertout C., 1991, A&A 252, 625
Berdyugin A.V., 1997, private communication
Berdyugina S.V., 1991, Izv. Krymsk. Astrofiz. Obs. 83, 102
Berdyugina S.V., Ilyin I., Tuominen I., 1998a, in preparation
Berdyugina S.V., Ilyin I., Tuominen I., 1998b, in preparation
Byrne P.B., Panagi P.M., Lanzafame A.C., et al., 1995, A&A 299, 115
Chugainov P.F., 1976a, Izv. Krym. Astrofiz. Obs. 54, 89
Chugainov P.F., 1976b, Izv. Krym. Astrofiz. Obs. 55, 85
Clegg R.E.S., Lambert D.L., Tomkin J., 1981, ApJ 250, 262
Davis S.P., Phillips J.G., 1963, The Red System ($A^2\Pi - X^2\Sigma$) of the CN molecule, University of California Press., Berkely
Dempsey R.C., Linsky J.L., Fleming T.A., Schmitt J.H.M.M., 1993, ApJS 86,599
Drake J.J., Smith G., 1991, MNRAS 250, 89
Drake S., Simon T., Linsky J.L., 1989, ApJS 71, 905
Eggen O.J., 1978, Inf. Bull. Variable Stars, 1426
Fekel F.C., 1996, In: Strassmeier K.G., Linsky J.L. (eds.) Proc. IAU Symp. 176, Stellar Surface Structure. Kluwer Acad. Publ., Dordrecht, p. 345
Fekel F.C., 1997, PASP 109, 514
Fekel F.C., Balachandran S., 1993, ApJ 403, 708
Fitzpatrick M.J. 1993, in: Hanish R., Brissenden R., Barnes J. (eds.) Astronomical Data Analysis Software and Systems II, ASP, San Francisco, p. 472
Giampapa, 1984, ApJ 277, 235
Glebocki R., Stawikowski A., 1995 Acta Astronomica 45, 725
Hadrava P., 1995, FOTEL3 - user's guide, Astronomical Institute, Academy of Science, Ondrejov
Halliday I., 1952, J.R.A.S. Canada 46, 103
Heard J.F., 1956, Publ. David Dunlap Obs. 2, 107
Henry G.W., Eaton J.A., Hamer J., Hall D.S., 1995, ApJ 97,513
Huenemoerder D.P., Ramsey L.W., 1987, ApJ 319, 392
Ilyin I.V., 1997, Licentiate Dissertation, University of Oulu
Jeffries R.D., Byrne P.B., Doyle J.G., et al., 1994, MNRAS 270, 153
Jetsu L., 1996, private communication
Kjaergaard P., Gustafsson B., Walker G.A.H., Hultqist L., 1982, A&A 115, 145
Kovacs I., 1969, The rotational Structure in the Spectra of Diatomic Molecules, Academiai Kiado, Budapest
Kurucz R.L., 1993, Kurucz CD No. 13

Kuznetzova L.A., Pazyuk E.A., Stolyarov A.V., 1993, Russ. J. Phys. Chem. 67, 2046
Lambert D.L., Ries L.M., 1981, ApJ 248, 228
Lang K.R., 1992, Astrophysical Data, Springer-Verlag
Martin E.L., Claret A., 1996, A&A 306, 408
Nations H.L., Ramsey L.W., 1981, AJ 85,1086
Neff J.E., O'Neal D., Saar S.H., 1995, ApJ 452, 879
O'Neal D., Neff J.E., 1997, AJ 113, 1129
Perryman M.A.C., Lindegren L., Kovalevsky J. et al., 1997, A&A 323, L49
Patterer R.J., Ramsey L., Huenemoerder D.P., Welty A.D., 1993, AJ 105, 1519
Piskunov N.E., Kupka F., Ryabchikova T.A., Weiss W.W., Jeffrey C.S., 1995, A&AS 112, 525
Randich S., Giampapa M.S., Pallavicini R.,1994,A&A 283,893
Rucinski S.M., 1977, PASP 89, 280
Sanford R.F., 1921, ApJ 53, 201
Scaltriti F., Piirola V., Coyne G.V., et al., 1993, A&AS 102, 343
Scarfe C.D., Batten A.H., Fletcher J.M. 1990, Publ. Dominion Astrophys. Obs. 18, 21
Schaerer D., Meynet G., Maeder A., Schaller G., 1993, A&AS, 98, 523
Stockton R.A., Fekel F.C., 1992, MNRAS 256, 575
Strassmeier K.G., Hall D.S., Fekel F.C., Scheck M., 1993, A&AS 100, 173
Tuominen I., 1992, Nordic Optical Telescope News 5, 15
Vogt S.S., 1981, ApJ 247, 975
Wolinski K.G., Dolan J.F., 1994, MNRAS 267, 5